

Reversible Association/Dissociation Reaction of Avidin on the Dendrimer Monolayer Functionalized with a Biotin Analogue for a Regenerable Affinity-Sensing Surface

Hyun C. Yoon, Mi-Young Hong, and Hak-Sung Kim*

Department of Biological Sciences, Korea Advanced Institute of Science and Technology, 373-1, Kusung-dong, Yuseong-ku, Taejeon 305-701, Korea

Received September 26, 2000. In Final Form: November 15, 2000

A new approach to a repeatedly regenerable affinity-sensing surface was developed based on the reversible association/dissociation reactions between avidin and biotin analogues. For the affinity surface, a fourth generation poly(amidoamine) dendrimer monolayer was first constructed on the 11-mercaptopoundecanoic acid self-assembled monolayer on gold. The dendritic surface amine groups then were functionalized with biotin analogues, desthiobiotin (**1**), or newly synthesized desthiobiotin amidocaproate (**2**), an extended form of **1**, which shows lower affinity toward avidin. To test the association/dissociation reaction cycles at the affinity surface, avidin adlayer was formed onto the biotin analogue functionalized surface and displaced with free biotin. To trace the stepwise reactions, biotinylated glucose oxidase (b-GOx) as a model enzyme was loaded onto the affinity surface, and cyclic voltammetric measurements were performed by registering the activity of the associated b-GOx. The efficient association/dissociation reaction cycles were registered, especially for the **2**-modified electrodes, implying steric hindrance from the ligand length for biospecific interaction. With the optimized affinity-surface construction steps and reaction conditions, continuous association/dissociation reaction cycles were achieved, resulting in a regenerable affinity surface.

Introduction

This paper describes an approach to developing repeatedly regenerable affinity biosensing surfaces, which is based on biospecific association and displacement interactions. We chose avidin–biotin couple as the model molecules for the protein–ligand interaction, because this couple is widely applied in the biorelated fields.¹ Also, we took advantage of the availability of several biotin analogues exhibiting various affinities toward (strept-)avidin molecules. For example, the association constant (K_a) for desthiobiotin toward streptavidin ($5 \times 10^{13} \text{ M}^{-1}$)^{2,3} is only a $1/20$ th of that for biotin to streptavidin or avidin molecules ($\sim 1 \times 10^{15} \text{ M}^{-1}$),^{2,4} which is the working principle of dissociation reaction by displacement.^{2,5}

There has been a growing interest in molecularly organized surfaces containing biomolecules for the purposes of immunoassays and DNA analyses,^{6–9} artificial biomimetic membranes,^{10–12} and bioelectronic devices.¹³

These applications mainly depend on the self-assembled monolayer (SAM) technology.¹⁴ The implementations of mixed SAMs^{15–17} and micropatterning method such as microcontact printing^{18–20} have expanded the applicability of the SAM-based structures. Furthermore, the developments of useful (bio-)functionalization methodologies of the constructs as well as the incorporations of novel materials representing unique properties are the subjects of intensive studies.^{21–27}

We previously reported the applications of molecularly organized cascade polymers, dendrimers,^{28–30} for the

* Corresponding author: phone, 82-42-869-2616; fax, 82-42-869-2610; e-mail, hskim@mail.kaist.ac.kr.

(1) Wilchek, M.; Bayer, E. A. *Anal. Biochem.* **1988**, *171*, 1–32.
 (2) Müller, W.; Ringsdorf, H.; Rump, E.; Wildburg, G.; Zhang, X.; Angermaier, L.; Knoll, W.; Liley, M.; Spinke, J. *Science* **1993**, *262*, 1706–1708.
 (3) Hoffmann, M.; Müller, W.; Ringsdorf, H.; Rourke, A. M.; Rump, E.; Suci, P. A. *Thin Solid Films* **1992**, *210/211*, 780–783.
 (4) Florin, E.-L.; Moy, V. T.; Gaub, H. E. *Science* **1994**, *264*, 415–417.
 (5) Måsson, M.; Yun, K.; Haruyama, T.; Kobatake, E.; Aizawa, M. *Anal. Chem.* **1995**, *67*, 2212–2215.
 (6) Jordan, C. E.; Frutos, A. G.; Thiel, A. J.; Corn, R. M. *Anal. Chem.* **1997**, *69*, 4939–4947.
 (7) Okahata, Y.; Kawase, M.; Niikura, K.; Ohtake, F.; Furusawa, H.; Ebara, Y. *Anal. Chem.* **1998**, *70*, 1288–1296.
 (8) Sekar, M. M. A.; Hampton, P. D.; Buranda, T.; López, G. P. *J. Am. Chem. Soc.* **1999**, *121*, 5135–5141.
 (9) Hofstetter, O.; Hofstetter, H.; Wilchek, M.; Schurig, V.; Green, B. S. *Nature Biotechnol.* **1999**, *17*, 371–374.
 (10) Cornell, B. A.; Braach-Maksyvtis, V. L. B.; King, L. G.; Osman, P. D. J.; Raguse, B.; Wiecezorek, L.; Pace, R. J. *Nature* **1997**, *387*, 580–583.
 (11) Moteshareh, K.; Ghadiri, M. R. *J. Am. Chem. Soc.* **1997**, *119*, 11306–11312.

(12) Peng, T.; Cheng, Q.; Stevens, R. C. *Anal. Chem.* **2000**, *72*, 1611–1617.
 (13) Liu, Q.; Wang, L.; Frutos, A. G.; Condon, A. E.; Corn, R. M.; Smith, L. M. *Nature* **2000**, *403*, 175–179.
 (14) Ulman, A. *An Introduction to Ultrathin Organic Films: From Langmuir–Blodgett to Self-Assembly*; Academic Press: Boston, 1991.
 (15) Boncheva, M.; Scheibler, L.; Lincoln, P.; Vogel, H.; Åkerman, B. *Langmuir* **1999**, *15*, 4317–4320.
 (16) Lahiri, J.; Isaacs, L.; Grzybowski, B.; Carbeck, J. D.; Whitesides, G. M. *Langmuir* **1999**, *15*, 7186–7198.
 (17) Pérez-Luna, V. H.; O'Brien, M. J.; Opperman, K. A.; Hampton, P. D.; López, G. P.; Klumb, L. A.; Stayton, P. S. *J. Am. Chem. Soc.* **1999**, *121*, 6469–6478.
 (18) Lahiri, J.; Ostuni, E.; Whitesides, G. M. *Langmuir* **1999**, *15*, 2055–2060.
 (19) Willner, I.; Schlittner, A.; Doron, A.; Joselevich, E. *Langmuir* **1999**, *15*, 2766–2772.
 (20) Ghosh, P.; Crooks, R. M. *J. Am. Chem. Soc.* **1999**, *121*, 8395–8396.
 (21) Mooney, J. F.; Hunt, A. J.; McIntosh, J. R.; Liberko, C. A.; Walba, D. M.; Rogers, C. T. *Proc. Natl. Acad. Sci. U.S.A.* **1996**, *93*, 12287–12291.
 (22) Caruso, F.; Rodda, E.; Furlong, D. N.; Niikura, K.; Okahata, Y. *Anal. Chem.* **1997**, *69*, 2043–2049.
 (23) Cosnier, S.; Stoytcheva, M.; Senillou, A.; Perrot, H.; Furriel, R. P. M.; Leone, F. A. *Anal. Chem.* **1999**, *71*, 3692–3697.
 (24) Dequaire, M.; Degrand, C.; Limoges, B. *J. Am. Chem. Soc.* **1999**, *121*, 6946–6947.
 (25) Anzai, J.; Kobayashi, Y.; Nakamura, N.; Nishimura, M.; Hoshi, T. *Langmuir* **1999**, *15*, 221–226.
 (26) Yoon, H. C.; Kim, H.-S. *Anal. Chem.* **2000**, *72*, 922–926.
 (27) Yoon, H. C.; Hong, M.-Y.; Kim, H.-S. *Anal. Chem.* **2000**, *72*, 4420–4427.
 (28) Newkome, C. R.; Moorefield, C. N.; Vögtle, F. *Dendritic Molecules. Concepts-Syntheses-Perspectives*; Springer-Verlag: New York, 1996.

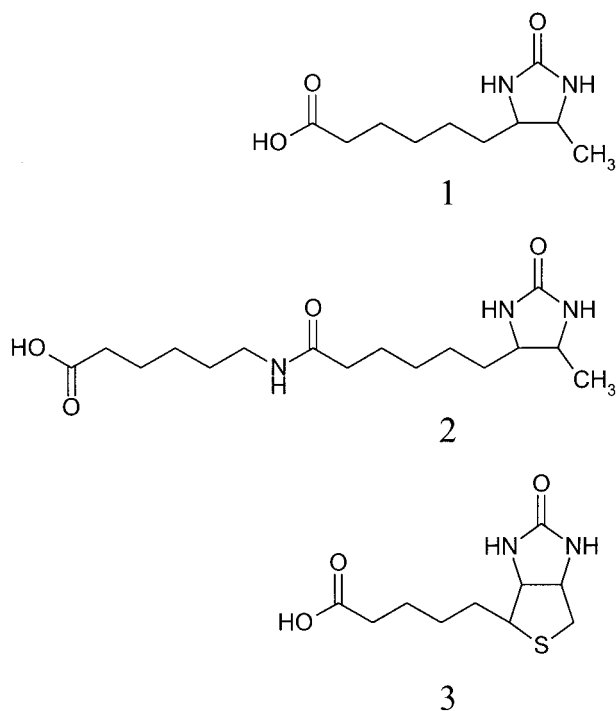


Figure 1. Molecular structures of d-desthiobiotin **1**, d-desthiobiotin amidocaproate **2**, and d-biotin **3**.

preparation of multilayered biocomposite nanostructures.^{26,27} A fourth generation (G4) poly(amidoamine) dendrimer was adopted as the building block for the multilayered enzyme biocomposite films for the biosensors. We have recently devised an affinity-sensing electrode based on the dendrimer monolayer and its functionalization with biospecific ligands.³¹ The dendritic surface was partly functionalized with ferrocenyl groups for efficient electrochemical signal generation in addition to the biospecific ligand groups, which was equivalent to the mixed SAMs.

Affinity-sensing surfaces find a great deal of utility in the separation of biomolecules, understanding of biomolecular interactions, and affinity biosensors. Developing an efficient method to regenerate the affinity surfaces has long been a subject of research but still remains to be further explored. For the dissociation of bound molecules from the sensing surfaces, treatments such as extreme pH, temperature adjustment, and chaotropic agents are available but often followed by a significant loss of biospecific activity.³² It should be noted that the majority of the developed affinity-sensing devices were originally designed as the one-shot, disposable type.

In this paper, we present a new strategy of developing a repeatedly renewable affinity-sensing surface. We employed biotin analogues **1** (desthiobiotin) and **2** (desthiobiotin amidocaproate, extended form of **1**) for surface functionalization and biospecific recognition reaction (Figure 1), and displacement dissociation for the regeneration of the affinity-sensing surface. The platform for the ligand functionalization was made with poly(amidoamine) dendrimers on 11-mercaptoundecanoic acid (MUA) SAM/Au electrode. Biospecific association reaction was performed with avidin, and the dissociation step was

conducted via displacement with free biotin, **3** (Figure 1). To test the reversibility of the process, biotinylated glucose oxidase (b-GOx) was loaded onto the avidin layer, and the enzyme activity was traced by using cyclic voltammetry at each reaction step. The affinity-sensing surface developed in this study exhibited effective biospecific association/dissociation reaction cycles, promising for the reversible affinity biosensor. Details are reported herein.

Experimental Section

Materials. The synthesis of compound **2**, desthiobiotin amidocaproate, is described below. Compounds **1** and **3** (Figure 1), D-(+)-glucose, 1-ethyl-3-(3-dimethylaminopropyl) carbodiimide hydrochloride (EDAC), and biotin-amidocaproyl labeled glucose oxidase (b-GOx, from *Aspergillus niger*, minimum 4 mol of biotin per mole of protein) were purchased from Sigma. 11-Mercaptoundecanoic acid and pentafluorophenol were purchased from Aldrich. *N,N,N,N*-tetramethyl-*O*-(*N*-succinimidyl)uronium tetrafluoroborate and 6-aminocaproic acid were obtained from Fluka. *N*-Hydroxysulfosuccinimide (sulfo-NHS) was purchased from Pierce. Amine-terminated fourth generation poly(amidoamine) dendrimers are manufactured by Dendritech, Inc. (Midland, MI) and were purchased from Aldrich. Avidin from hen egg white (Sigma) and immunopure avidin (Pierce) were used as received from manufacturers. All other materials used were of the highest quality available and purchased from regular sources. For the buffer solutions, doubly distilled and deionized water with a specific resistance over 18 M Ω cm was used throughout the work.

Apparatus. Cyclic voltammetric and chronocoulometric measurements were carried out with a BAS CV-50W electrochemical analyzer (W. Lafayette, IN). A standard three-electrode configuration with a gold thin-film working electrode, a platinum wire counter electrode, and an Ag/AgCl (3 M NaCl, BAS) reference electrode was used. All measurements were performed at room temperature (25 ± 2 °C) under argon atmosphere unless otherwise specified.

The ¹H NMR spectra were recorded on a Bruker AVANCE-400 (400 MHz) spectrometer with tetramethylsilane (TMS) as the internal standard ($\delta = 0.0$ ppm). Mass spectral data were obtained on an Autospec Ultima (Fisons Instrument, England) mass spectrometer.

Synthesis of Desthiobiotin-Amidocaproate, 2. This compound was prepared by reaction of desthiobiotin (5-methyl-2-oxo-4-imidazoline caproic acid, **1**) with 6-aminocaproic acid through an amide bond formation. First, **1** (107 mg, 0.5 mmol) was dissolved in 3 mL of 1:1:1 DMF/dioxane/H₂O (v:v:v). To this solution, diisopropylethylamine (257 μ L, 1.5 mmol) and *N,N,N,N*-tetramethyl-*O*-(*N*-succinimidyl)uronium tetrafluoroborate (TSTU, 190 mg, 0.63 mmol) were added. This reaction has been developed to activate the free carboxylic acid end groups.^{33,34} The reaction mixture was stirred for 20 min at room temperature. After this step, 6-aminocaproic acid (98 mg, 0.75 mmol) was added to the activated product mixture and stirred at room temperature. After 30 min, the solvent was removed under reduced pressure and the residue was dissolved in H₂O (10 mL). The aqueous solution was washed with CHCl₃ and then lyophilized to give the crude product. The crude product was purified by silica column chromatography (2 cm i.d., 20 cm in length) using CHCl₃ and a CHCl₃/MeOH mixture as eluents. The column-purified fractions were collected and evaporated to dryness, and the product was verified with thin-layer chromatography. The desired product, **2**, was eluted with 3:1 CHCl₃/MeOH (v:v) eluting solution. The product was identified by mass spectrometry and ¹H NMR spectroscopy. EI-MS: *m/z* 327.1968 (M⁺, C₁₆H₂₉N₃O₄ requires 327.1952). ¹H NMR δ _H (400 MHz, MeOH, 25 °C, TMS): 3.81(m, 1H), 3.68(m, 1H), 3.16(t, *J* = 7.0 Hz, 2H), 2.27(t, *J* = 7.4 Hz, 2H), 2.17(t, *J* = 7.0 Hz, 2H), 1.61(m, 4H), 1.48(m, 4H), 1.32–1.38(br, 6H), 1.09(d, *J* = 3.8 Hz, 3H).

Construction of the Dendrimer Monolayers on Gold Surfaces. The affinity-sensing monolayer was made on thin-

(29) Freemantle, M. *Chem. Eng. News* **1999**, 77 (44), 27–35.

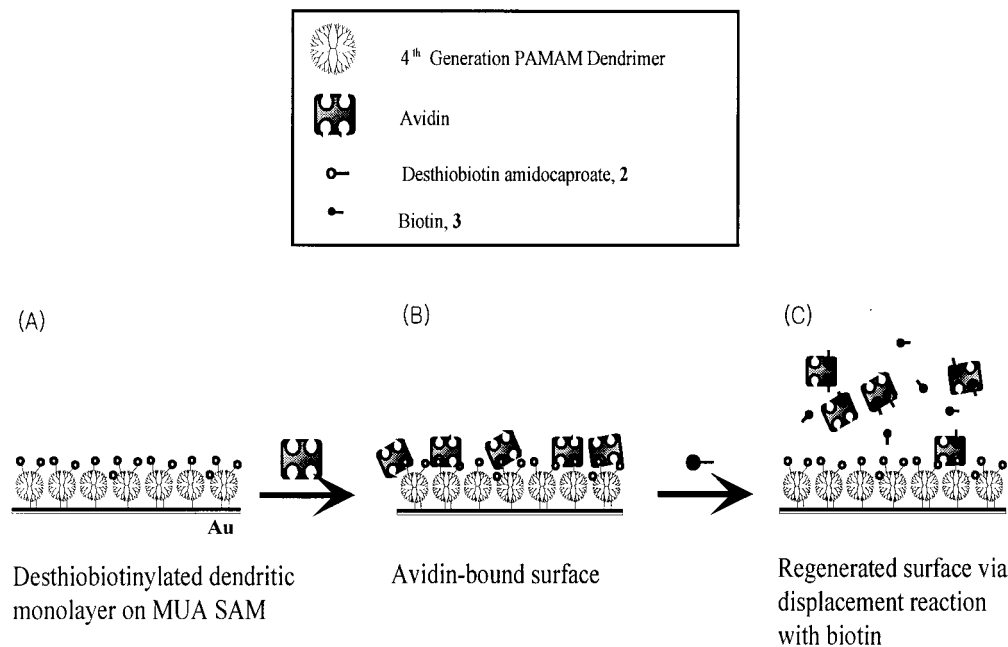
(30) Tsukruk, V. V. *Adv. Mater.* **1998**, 10, 253–257.

(31) Yoon, H. C.; Hong, M.-Y.; Kim, H.-S. *Anal. Biochem.* **2000**, 282, 121–128.

(32) Asanov, A. N.; Wilson, W. W.; Oldham, P. B. *Anal. Chem.* **1998**, 70, 1156–1163.

(33) Bannwarth, W.; Knorr, R. *Tetrahedron Lett.* **1991**, 32, 1157–1160.

(34) Singh, P. *Bioconjugate Chem.* **1998**, 9, 54–63.

Scheme 1. Schematic Representation of the Procedure Employed for the Biospecific Association/Dissociation of Biomolecules at the Affinity-Sensing Electrode Surfaces

film gold surface, prepared by resistive evaporation of 200 nm of Au (99.999%) onto titanium-primed (20 nm Ti) silicon wafers (Si(100)). Freshly prepared surfaces were used as base substrates for the fabrication of affinity-sensing monolayered electrodes. Prior to the layering process, the electrode surfaces were cleaned by immersing them (5 min) in piranha solution (1:4 by volume of 30% H_2O_2 and concentrated H_2SO_4). *CAUTION: piranha solution reacts violently with most organic materials and must be handled with extreme care.*

The bottom-up synthetic procedure for the affinity-sensing surfaces started with the introduction of SAMs representing reactive carboxylate groups on the gold surfaces. By the chemisorption of MUA (2 mM) in ethanol for 2 h, a carboxylate-ended SAM was prepared on gold electrodes. After the SAM formation and ethanol rinsing steps, the carboxylate groups were reacted with pentafluorophenol to give reactive ester groups toward amine functionalities from the G4 poly(amidoamine) dendrimers. The SAM-modified electrodes were immersed in a DMF solution containing EDAC (0.1 M) and pentafluorophenol (0.2 M). After the activation reaction for 20 min, the electrodes were rinsed with DMF, dried under an argon stream, and transferred to a dendrimer solution in methanol. The 10% (w/w) methanolic dendrimer solution was diluted to 0.25 mM (based on the dendrimer concentration, 5 mL) and was used for the formation of a dendrimer monolayer. After reaction for 30 min, the surfaces were rinsed with methanol, dried with a stream of argon, and immersed in a bicarbonate buffer (0.1 M, pH 9.5) for 30 min to hydrolyze the remaining reactive fluorophenyl esters. At this stage, the surface modification processes for the dendrimer monolayer on the gold electrode were completed, and the electrodes were stored in the bicarbonate buffer for further modification.

Surface Functionalization of Dendrimer Monolayers with Biotin Analogues. Before the desthiobiotinylation process, the electrodes were removed from the storage solution, rinsed, air-dried, and clamped to homemade Teflon electrode holders. The holders were designed to expose the defined electrode area of 0.148 cm^2 and the reaction well volume of 3 mL. Chronocoulometric measurement was employed for the determination of electrode area.

Surface functionalization reactions with biotin analogues were performed with either compound **1** or **2**. A HEPES buffer solution (0.01 M, pH 7.3) containing EDAC (0.04 M) and sulfo-NHS (0.025 M) was freshly prepared before use. This EDAC/sulfo-NHS solution was added to the prepared electrode holders. To this electrode-immersed solution, a methanolic solution of **1** or **2** (100 μL) was added dropwise and incubated overnight at room

temperature. The final concentration of desthiobiotins was adjusted to 0.02 M. After reaction was completed, the electrodes were rinsed with HEPES buffer and distilled water, and were stored in a phosphate-buffered saline solution (PBST, pH 7.4, 10 mM phosphate, 2.7 mM KCl, and 138 mM NaCl, 0.05% (v/v) Tween 20) prior to use.

Affinity Binding with Avidin and the Surface Regeneration via the Displacement Reaction with Biotin, 3. The idealized schematic representation for the affinity binding and displacement reaction steps at the electrode surface is depicted in Scheme 1. For the affinity interaction, we used avidin as a model molecule to the desthiobiotinyl-modified electrode surfaces. Aliquots of avidin samples (50 $\mu\text{g}/\text{mL}$, in PBST) were prepared and incubated at the electrode for 45 min at room temperature. After the surfaces were rinsed with PBST (30 s, 3 times), the avidin-modified layers were incubated with biotin—amidocaproyl labeled glucose oxidase (b-GOx, 0.5 mg/mL, in PBST) for 45 min at room temperature. The b-GOx was used for the direct electrochemical determination of the binding/displacement reactions occurring at the affinity surfaces (vide infra). After the electrochemical measurements, the displacement reaction was performed by exchanging the electrolyte with the solution of biotin (2 mM, in PBST) and incubating for 1 h. It should be noted that PBST rinsing followed all the reaction steps.

Electrochemical Tracing of Association/Dissociation Reactions. To trace the biospecific association of avidin onto the desthiobiotinyl-functionalized surface and the dissociation of avidin molecules via displacement reaction with d-biotin, we determined the bioelectrocatalytic signal (current) generated by bound b-GOx molecules onto the preformed, underlying avidin layer. After each reaction step (i.e., association of avidin, association of b-GOx onto the avidin layer, and the dissociation of avidin/b-GOx couple from the electrode surface via displacement reaction), the electrodes were subjected to cyclic voltammetric measurements in the presence of glucose (50 mM) as the enzyme substrate and ferrocenemethanol (0.1 mM) as an electron-transferring mediator. The glucose solutions were prepared with phosphate buffer (0.1 M, pH 7.2) and were allowed to mutarotate overnight before use. The electrolyte solution used was deoxygenated with argon bubbling (20 min) before each voltammetric run.

Results and Discussion

Construction of the Affinity-Sensing Surface: Functionalized Dendrimer Monolayers on Gold Electrodes. First, the protocol for the construction of a

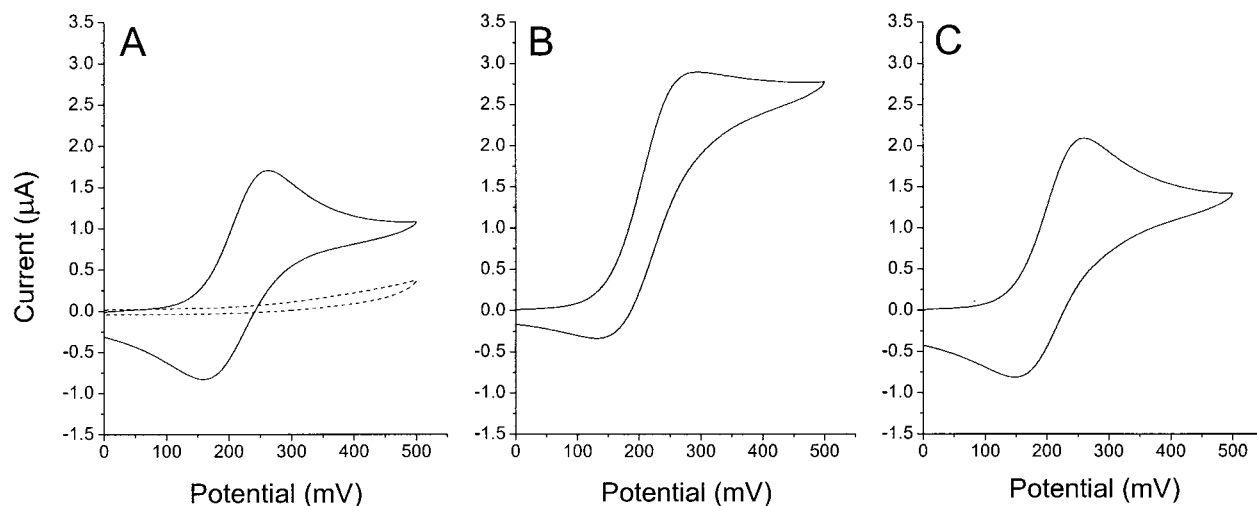


Figure 2. Cyclic voltammograms for the association/dissociation processes at the affinity surfaces: (A) freshly prepared and biotin-analogue-functionalized electrode surfaces in the presence (solid line) and absence (dashed line) of Fc-MeOH in electrolyte; (B) electrodes which were modified with avidin and further reacted with biotinylated glucose oxidase (b-GOx) in the presence of Fc-MeOH (0.1 mM) and glucose (50 mM); (C) electrode surfaces after displacement reaction with free biotin. All curves were shown for the affinity surfaces that were modified with desthiobiotin amidocaproate, compound **2**.

covalently modified dendritic monolayer on gold electrode surface was established. For the materialization of advantages anticipated from dendrimer use, such as stable and densely functionalizable platforms for the biospecific affinity interactions, construction of a highly organized and covalently modified dendritic monolayer is a prerequisite. A MUA-SAM was prepared, and the end-protruding carboxylate groups were activated with pentafluorophenyls via EDAC for this purpose. Introduction of pentafluorophenyl-activated ester groups as the reacting counterpart to the dendrimer surface amines resulted in much faster reaction, facilitating modification and further tethering processes. The amide bond forming reaction with pentafluorophenyl-activated ester groups has been found to be 10 times faster than with other active groups, e.g., succinimidyl esters.¹⁸ After the dendritic monolayer was constructed, the unreacted pentafluorophenyl ester groups were hydrolyzed to eliminate the possibility of undesired reactions during the successive processes. Formation of the dendritic monolayer was electrochemically verified by using the same method as previously reported for the electrode constructed with ferrocenyl-tethered dendrimers (Fc-Dend/MUA-SAM/Au).²⁷ From the cyclic voltammogram measurements for the Fc-Dend/MUA-SAM/Au electrode and the coulometric analysis, the amount of covalently immobilized ferrocenyl functionalities (surface density of immobilized ferrocenyls) can be estimated.²⁷ On the basis of the result, it was evident that the amine-terminated dendrimers are immobilized covalently onto MUA-SAM, forming a monolayer on the electrode surface.

After the formation of monolayer, the surface amine groups from dendrimers were further functionalized with biotin analogues, **1** (desthiobiotin) or **2** (desthiobiotin amidocaproate, extended form of **1**), via the amide bond formation reaction in the presence of EDAC/sulfo-NHS. At this point, construction of the affinity surfaces for the biospecific recognition of avidin was completed. Scheme 1 shows the stepwise reactions for the biospecific affinity binding and the surface regeneration via displacement reaction with biotin: (A) the freshly prepared electrode which was modified with a biotin analogue; (B) biospecific binding of avidin on the functionalized electrode surface; (C) the displacement reaction with biotin, the natural recognition couple to avidin. Biotin exhibits an association constant of $K_a = 1 \times 10^{15} \text{ M}^{-1}$, 20 times greater than that

of desthiobiotin, $K_a = 5 \times 10^{13} \text{ M}^{-1}$, by which the dissociation of bound avidin molecules is possible via displacement reaction.^{2,5}

Tracing of the association/displacement processes is based on the formation of biotinylated enzyme adlayer onto the avidin underlying layer with biotinylated glucose oxidase (b-GOx) and electrochemical determination of the activity of bound enzyme.

Electrochemical Characterization of the Biospecific Interactions: Affinity Binding of Avidin and the Surface Regeneration via Displacement Reaction with Biotin. Stepwise reactions involving association and displacement of avidin at the affinity surface were electrochemically traced. Cyclic voltammogram measurements were performed after each reaction step under the specified conditions (see Experimental Section).

Figure 2A shows the cyclic voltammograms for the freshly prepared electrode which was modified with desthiobiotin amidocaproate, in the presence (solid line) and absence (dashed line) of ferrocenemethanol in the electrolyte. The prepared gold electrode allowed a wide potential window for the efficient determination of bioelectrocatalysis and redox reaction of ferrocenyls. After the biospecific interaction with avidin and further association reaction with b-GOx on the avidin layer, the electrode showed a typical cyclic voltammogram for the ferrocenyl-mediated and enzyme-catalyzed reaction in the presence of both glucose and ferrocenemethanol as the enzyme substrate and electron-transferring mediator, respectively (Figure 2B). The currents from the bioelectrocatalysis at the electrode were registered as anodically amplified sigmoidal curves, and they reached a plateau at +290 mV vs Ag/AgCl. The electrode that had not been reacted with b-GOx after avidin association showed an almost identical voltammogram to that in Figure 2A (data not shown), indicating that the amplified current is due to the bound enzymes and that the avidin-associated layer retains its initial permeability. We believe that this consistent permeability is attributable to the use of dendrimers as the building unit for the affinity layer. In other words, the use of dendritic monolayer as the platform for the ligand functionalization prevents direct association of avidin molecules to the electrode surface or onto the rather short and crowded alkanethiol layer, which might take place in the case of an affinity surface constructed

Table 1. Assessment of the b-GOx Active Coverage during the Biorecognitive Adsorption of b-GOx on the Preformed Avidin Layer and the Displacement Routine of Underlying Avidin Layer by Biotin Added in Solution

association/displacement reaction cycle no.	$\Gamma_{\text{GOx,ON}}$ (10^{-13} mol cm^{-2})	$\Gamma_{\text{GOx,OFF}}$ (10^{-13} mol cm^{-2})
1	1.7 ± 0.1	0.8 ± 0.1
2	1.5 ± 0.2	0.6 ± 0.1
3	1.6 ± 0.2	0.6 ± 0.1
4	1.5 ± 0.1	

directly on functionalized alkanethiol SAM. Figure 2C represents the cyclic voltammogram for the electrode after the displacement reaction with biotin, the natural biospecific binding counterpart to avidin. The voltammogram was almost identical to that of the unmediated one shown in Figure 2A, indicating effective dissociation of avidin/b-GOx couple from the affinity surface. Meanwhile, the anodic peak current was a little higher than the original unmediated signal, which is due to the presumption that associated avidin molecules were not completely displaced and/or there might be nonspecific binding of enzymes to the surface. The influence of these aberrations was estimated below 15% to the signals from biospecific recognition reactions.

At the initial phase of the study, a set of affinity surfaces was prepared by using desthiobiotin, **1**, as the biospecific recognition moiety on the dendrimer monolayer. When the electrode surfaces were subjected to successive association reactions with avidin and b-GOx, voltammograms for the mediated and enzyme-catalyzed reaction were obtained, but the current levels were significantly lower in comparison to those from **2**-functionalized electrodes (Figure 2B and Table 1, *vide infra*). Furthermore, regeneration of the surface was not evident even after prolonged displacement reaction with biotin. We just observed a gradual decrease in anodic currents when measured continuously from the same electrode, and this seems to be caused by nonspecific binding of enzyme at the electrode surface and subsequent unfolding deactivation.³⁵

Amine-terminated G4 poly(amidoamine) dendrimers have a high $\text{p}K_{\text{a}}$ value of ca. 9.5,³⁶ and the dendrimer monolayer should exhibit positive surface charges under the reaction condition used (pH 7.4). Thus, nonspecific adsorption of avidin to the dendrimer monolayer would not be significant, because avidin molecules (isoelectric point of 10–10.5) are also positively charged under the same conditions, rejecting each other via charge repulsion. Meanwhile, glucose oxidase ($\text{pI} = 4.05$) possesses negative charges at pH 7.4 and can be adsorbed nonspecifically to the dendrimer monolayer through charge attraction. Therefore, it is supposed that inefficient regeneration of the **1**-modified surfaces is mainly due to the irreversible nonspecific binding of b-GOx onto the dendrimer monolayer without the formation of an intervening avidin layer. That is, after the b-GOx adlayer formation step for the **1**-modified electrode, there might be only nonspecifically adsorbed enzyme layer on the electrode surface, because nonspecific binding of avidin is negligible due to the repulsive charge interaction between avidin and dendrimer monolayer.

On the basis of the above considerations, we thought that the observed inefficiency in biospecific association/displacement reaction for the **1**-modified surface would be attributable to the low binding level of avidin molecules

to the **1** functionalities. If the intervening avidin layers were successfully formed through biospecific interaction, the b-GOx would also bind via the biospecific avidin–biotin recognition rather than nonspecific adsorption, since the avidin–biotin recognition is the most favorable biological affinity interaction known.¹ In this regard, it is supposed that there exists a severe steric hindrance for avidin molecules to specifically bind to the **1**-functionalized surface. It has been known that for the biospecific binding of biotin to avidin, several hydrogen bonds are generated for the tight recognition and they are formed universally from the ureido oxygen group with the Tyr-33 in the avidin-binding pocket and to the distal carboxylate oxygens of biotin.³⁷ From this, we reasoned that biotin analogues with extended chain length might offer more favorable configuration for the biospecific interaction with avidin, alleviating the steric hindrance, especially in the case of recognition events on the modified electrode surface.

With the electrode functionalized with compound **2**, the stepwise association/displacement (dissociation) reactions were successfully achieved. On the basis of the results, we attempted a repeatedly regenerable affinity-sensing surface by using the same approach as described above.

Repetitive Association/Displacement Reaction Cycles. A set of affinity-sensing surfaces, which was functionalized with compound **2**, was prepared and applied for the repetitive association/displacement processes. Cyclic voltammetric measurements were conducted after each reaction step, essentially with the same procedure as in Figure 2. For the convenient analysis of the data, signals were registered after normalization as follows. The anodic plateau signal, which was sampled from the voltammogram for the first association of avidin and successive association of b-GOx onto the freshly prepared electrode (“ON 1”), was denoted as I_{peak} . The anodic peak current from the unmediated voltammogram in the presence of ferrocenemethanol was measured as I_{back} . Finally, the anodic peak currents from the cyclic voltammograms at each measurement step were registered as I_{sig} . The normalized responses from the electrodes were calculated using the following equation.

$$\text{normalized response (\%)} = \frac{I_{\text{sig}} - I_{\text{back}}}{I_{\text{peak}} - I_{\text{back}}} \times 100\%$$

The “ON” and “OFF” signals obtained for the **2**-functionalized electrode surfaces through iterative biospecific association/dissociation reaction cycles are plotted in Figure 3. Evidently, the electrodes exhibited well-developed and reproducible association (“ON”)/dissociation (“OFF”) responses, confirming efficient biospecific interactions at the surfaces. The normalized responses oscillated between ca. 95% and 33%, for the associated and regenerated electrodes, respectively, and the signal fluctuations remained within 10% levels. Additionally, when a set of electrodes was tested after having been used and stored overnight in PBST, the electrodes responded normally through repeated regeneration cycles.

However, it should be noted that the signals from the displaced surfaces (“OFF” signal) did not return to the background level. The residual currents after displacement reaction steps were found to be about 33% (normalized signal), but these currents remained almost constant during the successive reaction cycles. We therefore thought that the phenomenon resulted from the incomplete displacement reaction. That is, there still existed a portion

(35) Seigel, R. R.; Harder, P.; Dahint, R.; Grunze, M.; Josse, F.; Mrksich, M.; Whitesides, G. M. *Anal. Chem.* **1997**, *69*, 3321–3328.

(36) Technical data supplied by Dendritech, Inc.

(37) Livnah, O.; Bayer, E. A.; Wilchek, M.; Sussman, J. L. *Proc. Natl. Acad. Sci. U.S.A.* **1993**, *90*, 5076–5080.

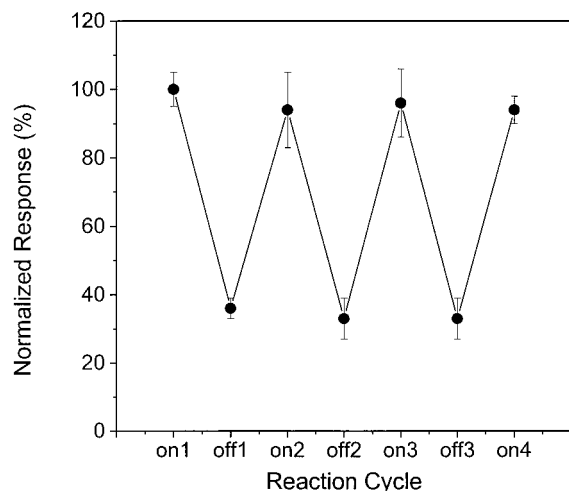


Figure 3. "ON" and "OFF" signal traces from the affinity surfaces via biospecific association/dissociation reaction cycles. Normalized signal levels were registered as $[(I_{\text{sig}} - I_{\text{back}})/(I_{\text{peak}} - I_{\text{back}})] \times 100$ (%).

of bound avidin/b-GOx even after the regeneration step. This incomplete displacement could be attributable to the bivalent binding of avidin onto the biotin-analogue-functionalized surface.¹⁷ Another possible explanation would be the nonspecific binding of enzyme at the surface. However, this scenario is not likely, because the residual signals were essentially maintained at a constant level during the successive association/dissociation cycles. If the nonspecific binding prevails, a gradual increase in the residual current might be expected (but not observed throughout the experiments). Thus, it is likely that the biospecific association/dissociation reactions take place efficiently at the affinity surface, even though there is an inherent limitation attributable to the tight bivalent binding of a portion of avidin to the functionalized surface.

To characterize and quantify the biospecific interaction at the surface, the responses at the electrodes were kinetically analyzed and tabulated (Table 1). The active b-GOx coverage at each reaction step was estimated from

kinetic analysis of voltammetric data on the basis of previous works of Savéant's group^{38,39} and ours.²⁶ As a result, the surface concentrations of active b-GOx were estimated to be ca. 1.6×10^{-13} and 0.6×10^{-13} mol·cm⁻² for the associated and regenerated electrodes, respectively. When the occupied area of a GOx molecule is considered to be about 100 nm²/enzyme, the calculated density for the compact monolayer corresponds to 1.7×10^{-12} mol·cm⁻².⁴⁰ Therefore, it was presumed that about 10% of the surface area was covered by proteins via biospecific recognition. This relatively low coverage seems to be caused by low functionalization yield of desthiobiotin at the electrode surface and the rather lower affinity of desthiobiotin toward avidin than biotin as previously stated. However, it should be noted that the affinity surface responded reversibly with a sufficient reproducibility during the repetitive association/dissociation reaction cycles.

In this study, we have demonstrated an effective approach to a repeatedly regenerable affinity-sensing surface, which is based on the interaction between avidin and a biotin analogue. The present method seems to be highly desirable for immunosensing and might be directly applicable to the affinity-based separation such as affinity chromatography. In addition, we believe that dendrimers are promising as the building units for the development of structurally organized and highly functionalized surface nanostructures.

Acknowledgment. This work was supported by the BK21 Program of the Ministry of Education and the National Research Laboratory Program of the Ministry of Science and Technology, Korea.

LA001373G

(38) Anicet, N.; Anne, A.; Moiroux, J.; Savéant, J.-M. *J. Am. Chem. Soc.* **1998**, *120*, 7115–7116.

(39) Bourdillon, C.; Demaille, C.; Moiroux, J.; Savéant, J.-M. *J. Am. Chem. Soc.* **1995**, *117*, 11499–11506.

(40) Franchina, J. G.; Lackowski, W. M.; Dermody, D. L.; Crooks, R. M.; Bergbreiter, D. E.; Sirkar, K.; Russell, R. J.; Pishko, M. V. *Anal. Chem.* **1999**, *71*, 3133–3139.